

SUPPLEMENTARY INFORMATION

Sol-Gel Based Structural Design of Macropores and Material Shapes of Metal–Organic Framework Gels

Yosuke Hara,^{a*} Kohei Manabe,^a Kazuki Nakanishi,^{b,c} and Kazuyoshi Kanamori^{a*}

^{a.} Department of Chemistry, Graduate School of Science Kyoto University Kitashirakawa, Sakyo-ku, Kyoto 606-8502 (Japan)

^{b.} Institute of Materials and Systems for Sustainability Nagoya University Furo-cho, Chikusa-ku, Nagoya, Aichi 464-8601 (Japan)

^{c.} Institute for Integrated Cell-Material Sciences, Kyoto University Yoshida, Sakyo-ku, Kyoto 606-8501 (Japan)

Email: hara.yosuke@icm.kyoto-u.ac.jp; kanamori@kuchem.kyoto-u.ac.jp

Table of Contents

S1. Experiment: Chemicals and Materials

S2. Experiment: Materials Synthesis

S3. Experiment: Physical Characterizations

S4. Results and Discussion

S5. References

S1. Experiment: Chemicals and Materials

Chromium(III) nitrate nonahydrate ($\text{Cr}(\text{NO}_3)_3 \cdot 9\text{H}_2\text{O}$) (>99%), polytetrahydrofuran (PTHF, $M_n = 2900$), poly(propylene glycol) (PPG, $M_n = 1000$ and 4000) were purchased from Sigma-Aldrich Co. LLC. (USA). Zirconium chloride octahydrate ($\text{ZrOCl}_2 \cdot 8\text{H}_2\text{O}$) ($\geq 99\%$) was purchased from FUJIFILM Wako Pure Chemical Co. (Japan). Formic acid (98~100%), *N,N*-dimethylformamide (DMF) ($\geq 99.5\%$), acetone ($\geq 99\%$), 2-propanol ($\geq 99.5\%$), ethanol ($\geq 99.5\%$), tetrahydrofuran ($\geq 99.5\%$), *n*-hexane ($\geq 99.5\%$), and toluene ($\geq 99.5\%$) were purchased from Kishida Chemical Co. (Japan). 1,3,5-Benzenetricarboxylic acid (BTC) ($\geq 98.0\%$) was purchased from Tokyo Chemical Industry Co. (Japan). Dimethyloctadecylchlorosilane ($\geq 97\%$) was purchased from Gelest, Inc. (USA).

S2. Experiment: Materials Synthesis

S2.1 Synthesis of macroporous Cr-BTC gels: A given amount of PTHF or PPG was dissolved in mixture of 13 mL of ethanol and tetrahydrofuran (1:1 vol%) at room temperature (25 °C). BTC (1.68 g) was subsequently added to obtain homogeneous solution at room temperature. After BTC was completely dissolved, $\text{Cr}(\text{NO}_3)_3 \cdot 9\text{H}_2\text{O}$ (4.80 g) was added into the solution, and stirred for 1 h at room temperature. After $\text{Cr}(\text{NO}_3)_3 \cdot 9\text{H}_2\text{O}$ was completely dissolved, the mixture was stirred in a water bath at 60 °C for 10 min until the mixture became homogeneous and transparent. Then, the solution was transferred into the preheated (60 °C) hydrophobic glass tubes by using a preheated (60 °C) pipette. (Hydrophobic glass tubes ($\phi 10$ mm: inside diameter is 8 mm) were prepared by the following process. The glass tubes with one side sealed were filled with 5 vol% toluene solution of dimethyloctadecylchlorosilane, and kept at 80 °C for 1 d. Then, the glass tubes were washed with acetone three times thoroughly and dried at 60 °C.) The glass tubes were sealed and kept at 60 °C in a water bath for **12 h** for gelation and aging. We used the glass tubes for synthesis of Cr-BTC monoliths. For synthesis of Cr-BTC microparticles, we used the glass bottles instead of glass tubes. (**Caution: The mixture of alcohol and nitric acid has potential explosively. Do not keep the solution at higher temperature above 80°C**). The obtained wet gels were kept at room temperature for 24 h for additional aging. The obtained wet gel was washed with ethanol and *n*-hexane glass bottle at 60 °C and 50 °C for 12 h three times and twice, respectively. The washed gel was dried at 40 °C in a loosely capped glass bottle to allow slow evaporation of *n*-hexane. Xerogels thus obtained were further dried at 80 °C, and then at 150 °C in a vacuum condition.

S2.2 Synthesis of non-macroporous Cr-BTC gels: BTC (1.68 g) was dissolved in mixture of 13 mL of ethanol and tetrahydrofuran (1:1 vol%) at room temperature (25 °C). After BTC was completely dissolved, $\text{Cr}(\text{NO}_3)_3 \cdot 9\text{H}_2\text{O}$ (4.80 g) was added into the solution, and stirred for 1 h at room temperature. After $\text{Cr}(\text{NO}_3)_3 \cdot 9\text{H}_2\text{O}$ was completely dissolved, the mixture was stirred in a water bath at 60 °C for 10 min. Then, the solution was transferred into the preheated (60 °C) hydrophobic glass tubes. The glass tubes were sealed and kept at 60 °C in a water bath for **24 h** for gelation and aging. The obtained wet gels were kept at room temperature for 24 h for additional aging. The obtained wet gel was washed with ethanol and *n*-hexane in a glass bottle at 60 °C and 50 °C for 12 h three times and twice, respectively. The washed gel was dried at 40 °C in a loosely capped glass bottle to allow slow evaporation of *n*-hexane. Xerogels thus obtained were further dried at 80 °C, and then at 150 °C in a vacuum condition.

S2.3 Synthesis of (non-)macroporous Zr-BTC gels: A given amount of PPG was dissolved in a mixture of DMF (4.0 mL) and formic acid (4.0 mL) at room temperature (25 °C). $\text{ZrOCl}_2 \cdot 8\text{H}_2\text{O}$ (3.22 g) was subsequently added to obtain homogeneous solution at room temperature. After $\text{ZrOCl}_2 \cdot 8\text{H}_2\text{O}$ was completely dissolved, BTC (0.70 g) was added into the solution, and stirred for 3-4 h at room temperature. After BTC was completely dissolved, the mixture was transferred into the hydrophobic glass tubes (\varnothing 8 mm: inside diameter is 6 mm) at room temperature. Then, the glass tubes were sealed and kept at 60 °C in a water bath for 12 h for gelation and aging. The obtained wet gel was washed with DMF, 2-propanol, and *n*-hexane at 80 °C, 60 °C, and 50 °C for 12 h twice, respectively. The washed gel was dried at 40 °C in a loosely capped glass bottle to allow slow evaporation of *n*-hexane. Xerogels thus obtained were further dried at 80 °C, and then at 120 °C in a vacuum condition.

S2.4 Synthesis of conventional MIL-100(Cr) particles: Conventional MIL-100(Cr) particles were synthesized according to the reported procedure with minor modifications. $^{11}\text{CrCl}_3 \cdot 6\text{H}_2\text{O}$ (1.05 g) and BTC (0.42 g) were mixed and ground by hand for 20 min at room temperature (25 °C). Then, the mixture in a Teflon-lined autoclave was placed in a preheated oven (220 °C) for 15 h. The obtained powder was washed with DMF and ethanol at 80 °C, and 60 °C for 12 h three times, respectively. The washed particles were dried at 80 °C. As-dried particles thus obtained were further dried at 150 °C in a vacuum condition.

S2.5 Synthesis of conventional MOF-808 particles: Conventional MOF-808 particles were synthesized according to the reported procedure with minor modifications. $^{12}\text{ZrOCl}_2 \cdot 8\text{H}_2\text{O}$ (0.16 g) and BTC (0.11 g) were dissolved in a solvent mixture of DMF/formic acid (20 mL/20 mL) at room temperature (25 °C). Then, the mixture was placed in a preheated oven (100 °C) for 2 d. The obtained powder was washed with DMF and ethanol at 80 °C, and 60 °C for 12 h three times, respectively. The washed particles were dried at 80 °C. As-dried particles thus obtained were further dried at 150 °C in a vacuum condition.

S3. Experiment: Physical Characterizations

The microstructures and element distributions of the fractured surfaces of the samples were investigated using a scanning electron microscope (SEM: JSM-IT500HR, JEOL Co., Japan, and JSM-6060S, JEOL Co., Japan) equipped with an energy dispersive X-ray spectroscopy (EDS). The surface of the samples was coated with Pt using an ion sputter (MC1000, Hitachi Co., Japan) prior to the observation. Macropore size distributions were measured by mercury porosimetry (AutoporeIV 9505, Shimadzu Co., Japan). All of the samples were degassed under vacuum at 150 °C (Cr-BTC gels) or 120 °C (Zr-BTC gels) overnight prior to the mercury porosimetry measurement. The thermal properties of the samples were investigated by thermogravimetry-differential thermal analysis (TG-DTA: TG-DTA 8122, Rigaku Co., Japan) with a continuous air supply at 100 mL min⁻¹. The crystal structure was examined by powder X-ray diffraction (XRD: RINT Ultima III, Rigaku Co., Japan) using Cu K α (λ = 0.154 nm) radiation as an incident beam. Micro-/Mesoporous structures of the samples were characterized by nitrogen adsorption-desorption (BELSORP-mini II and BELSORP-max, MicrotracBEL Corp., Japan). Sorption isotherms and BJH measurement were characterized by using BELSORP-mini II. Non-local density functional theory (NLDFT) measurements were characterized by using BELSORP-max and its analysis software BELMaster with assumption of N₂-carbon at 77 K on a slit pore model. All the samples were degassed under vacuum at 150 °C (Cr-BTC gels and conventional

SUPPLEMENTARY INFORMATION

MIL-100(Cr) particles) or 120 °C (Zr-BTC gels and conventional MOF-808 particles) overnight prior to the nitrogen adsorption-desorption measurement. The uniaxial compression tests on the samples were carried out using a material tester (Autograph AG-X plus, Shimadzu Corp., Japan). A cylindrical gel with a diameter 5 mm and a height of 5 mm was used for the compression tests.

S4. Results and Discussion

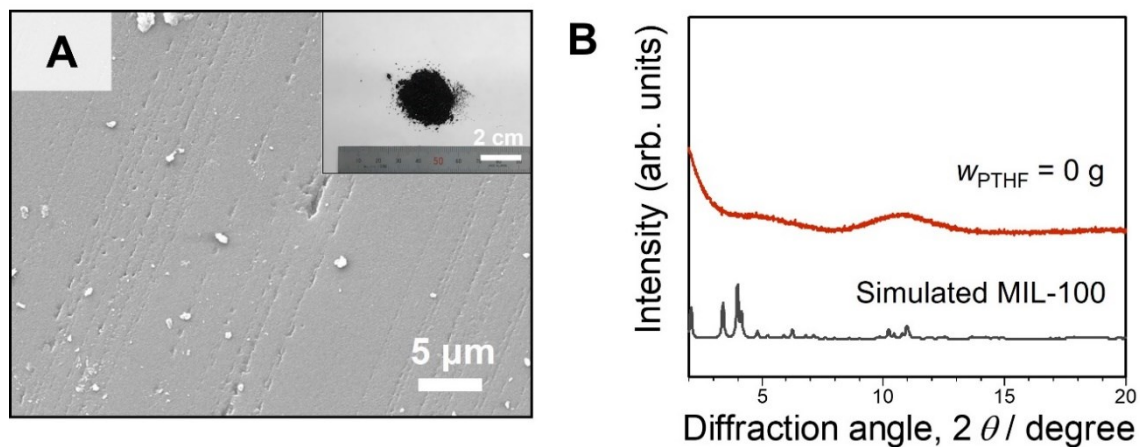


Figure S1. (A) An SEM image and appearance of the as-dried non-macroporous Cr-BTC gel: $w_{\text{PTHF}} = 0$ mg. (B) An XRD pattern of the same Cr-BTC gel.

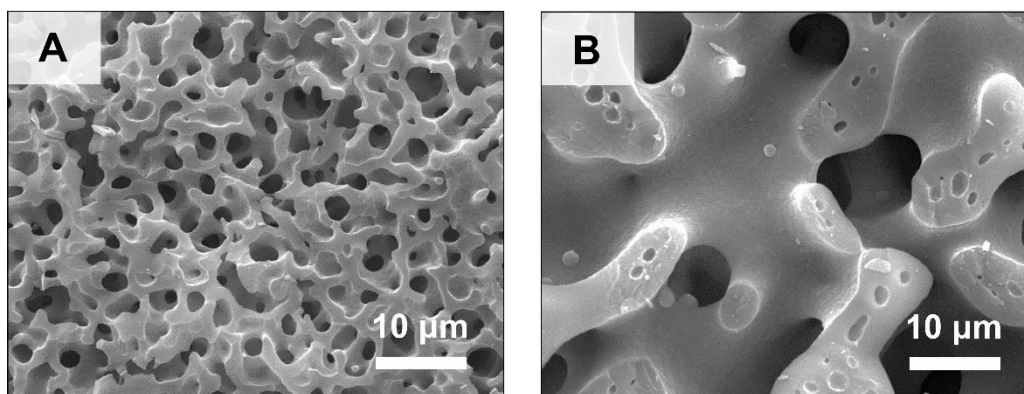


Figure S2. SEM images of the as-dried macroporous Cr-BTC gels prepared with varied amounts of PTHF: $w_{\text{PTHF}} =$ (A) 1.1 g (B) 1.3 g.

SUPPLEMENTARY INFORMATION

Table S1. Pore properties of the as-dried Cr-BTC gels.

sample	$d_{\text{macro}}^{\text{a}}/\mu\text{m}$	$S_{\text{BET}}^{\text{b}}/\text{m}^2 \text{g}^{-1}$	$V_{(\text{BJH})\text{pore}}^{\text{c}}/\text{cm}^3 \text{g}^{-1}$	$\rho_{\text{b}}^{\text{d}}/\text{g cm}^{-3}$
$w_{\text{PTHF}} = 1.1 \text{ g}$	1.3	661	0.11	0.42
$w_{\text{PTHF}} = 1.2 \text{ g}$	3.0	653	0.10	0.43
$w_{\text{PTHF}} = 1.3 \text{ g}$	-	657	0.10	-

[a] Modal pore size determined by mercury porosimetry. [b] Specific surface area obtained by the BET method.

[c] Mesopore volume obtained by the BJH method. [d] Bulk density obtained by mercury porosimetry.

SUPPLEMENTARY INFORMATION

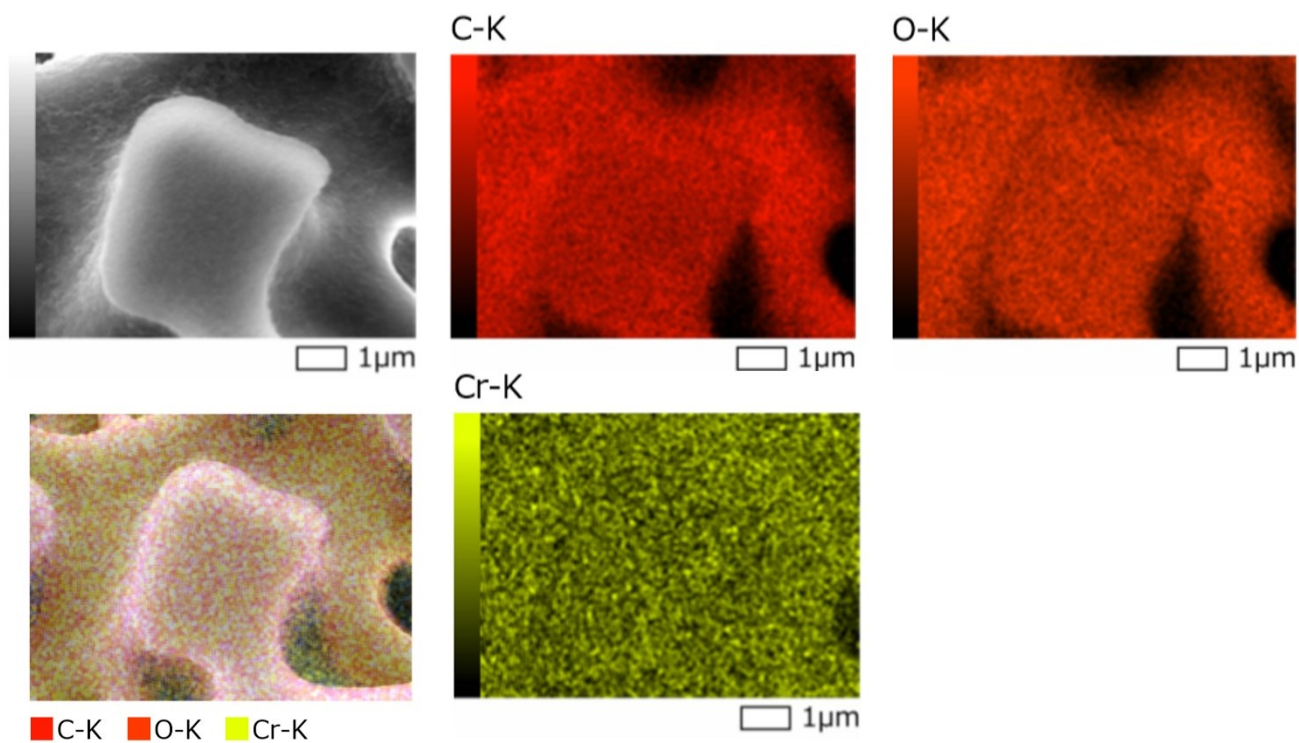


Figure S3. EDS element mapping results of the as-dried macroporous Cr-BTC gel: $w_{\text{PTHF}} = 1.2 \text{ g}$.

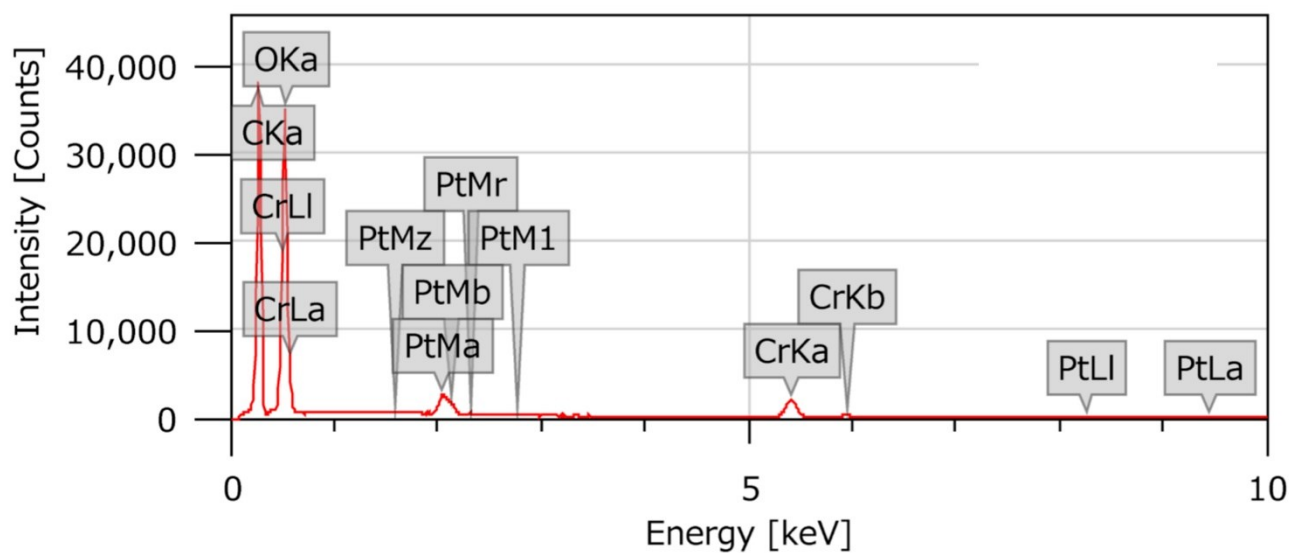


Figure S4. EDS spectrum of the as-dried macroporous Cr-BTC gel: $w_{\text{PTHF}} = 1.2 \text{ g}$. The surface of the sample was coated with Pt by ion sputtering.

SUPPLEMENTARY INFORMATION

Table S2. EDS element quantification result of the as-dried macroporous Cr-BTC gels ($w_{\text{PTHF}} = 1.2$ g).

Element	line	Mass%	Atom%
C	K	35.70 ± 0.03	50.53 ± 0.05
O	K	38.67 ± 0.07	41.09 ± 0.07
Cr	K	25.64 ± 0.18	8.38 ± 0.06
Summary	-	100.00	100.00

SUPPLEMENTARY INFORMATION

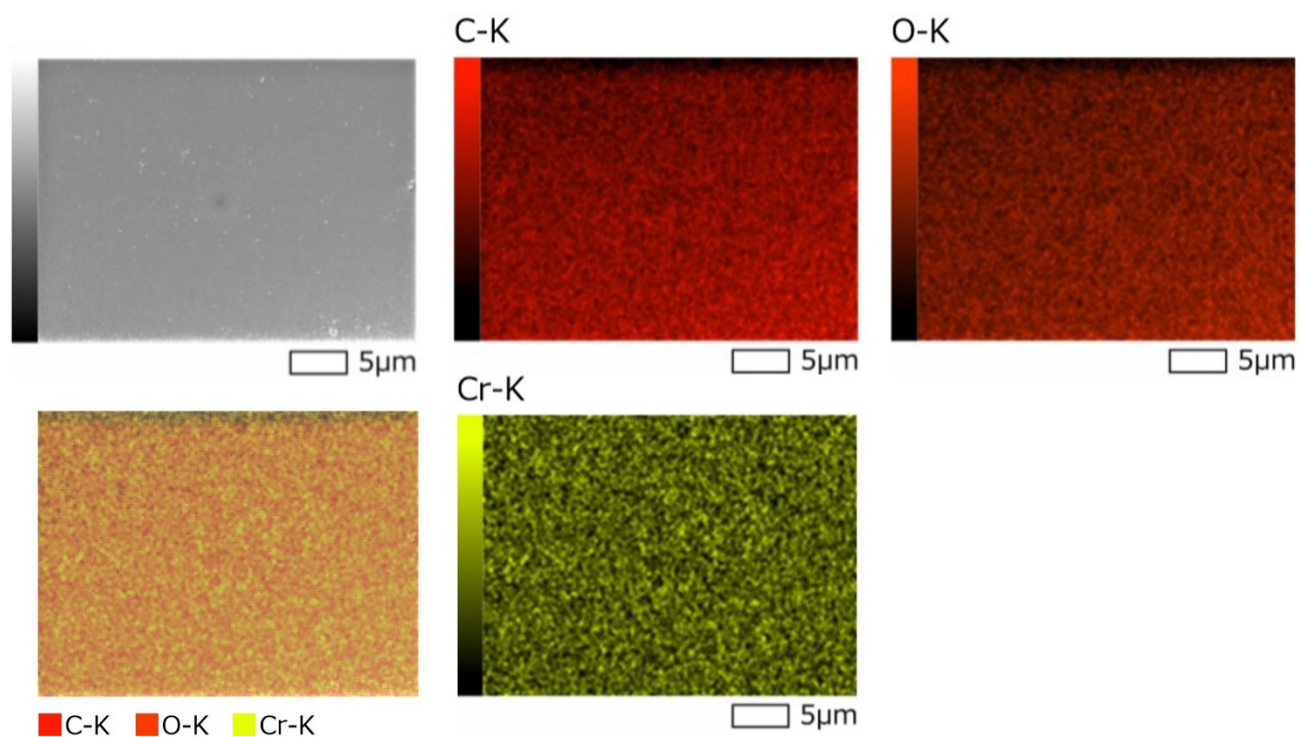


Figure S5. EDS element mapping results of the as-dried non-macroporous Cr-BTC gel: $w_{\text{PTHF}} = 0$ g.

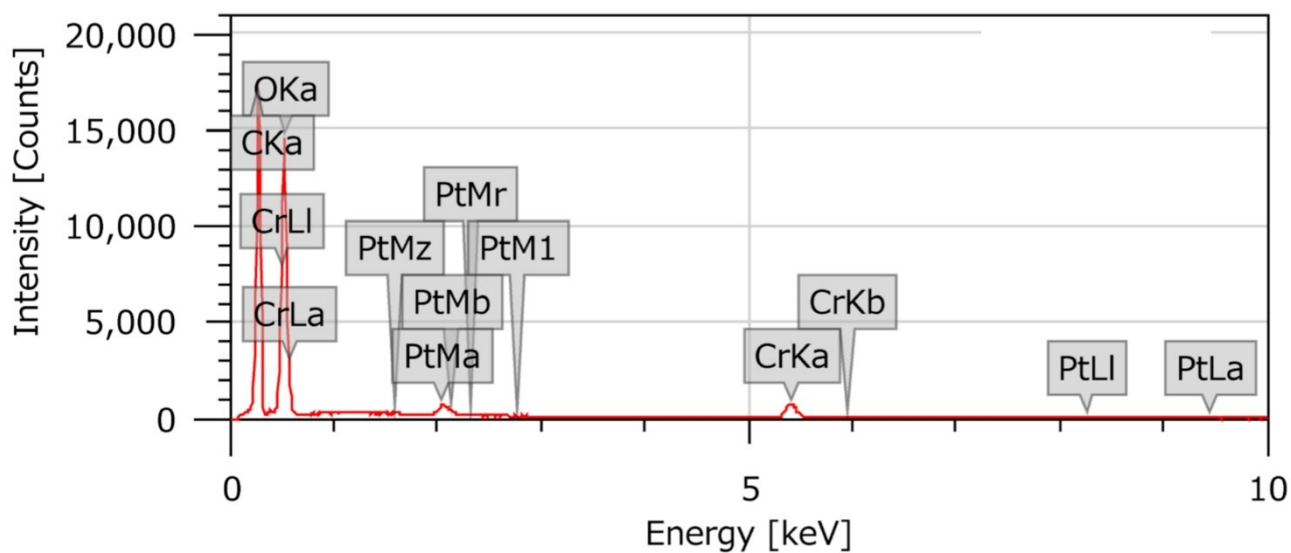


Figure S6. EDS spectrum of the as-dried non-macroporous Cr-BTC gel: $w_{\text{PTHF}} = 0$ g. The surface of the sample was coated with Pt by ion sputtering.

SUPPLEMENTARY INFORMATION

Table S3. EDS element quantification result of the as-dried macroporous Cr-BTC gel ($w_{\text{PTHF}} = 1.2$ g).

Element	line	Mass%	Atom%
C	K	38.14 ± 0.06	52.27 ± 0.08
O	K	39.52 ± 0.11	40.66 ± 0.11
Cr	K	22.34 ± 0.26	7.07 ± 0.08
Summary	-	100.00	100.00

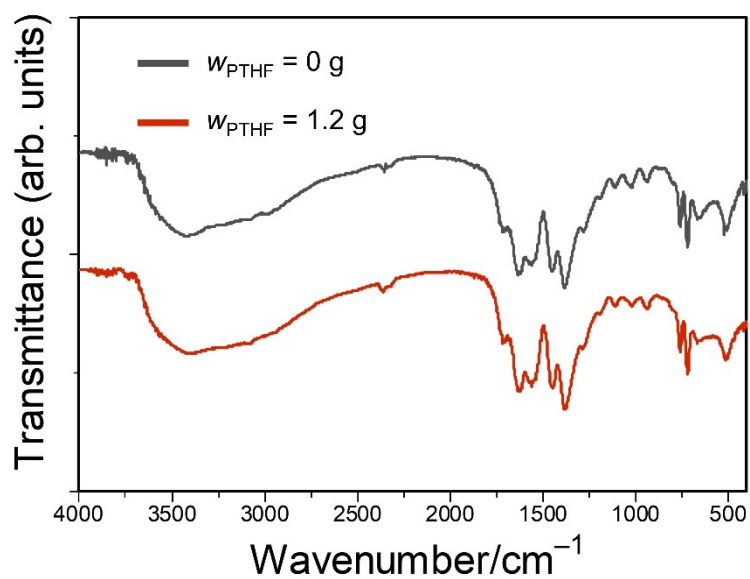


Figure S7. FTIR spectra of the as-dried Cr-BTC gels prepared with (1.2 g) and without PTHF.

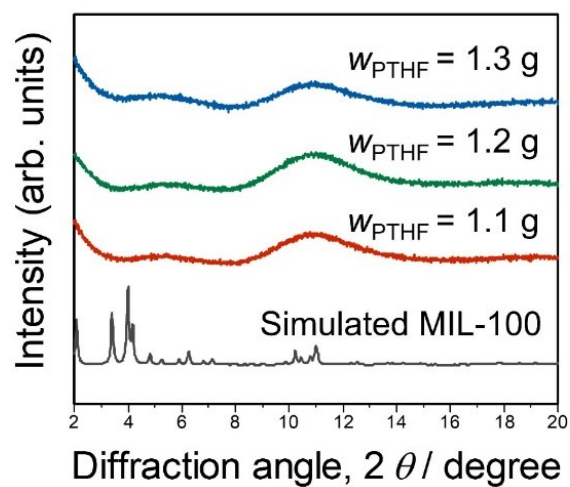


Figure S8. XRD patterns of the as-dried macroporous Cr-BTC gels with varied amounts of PTHF.

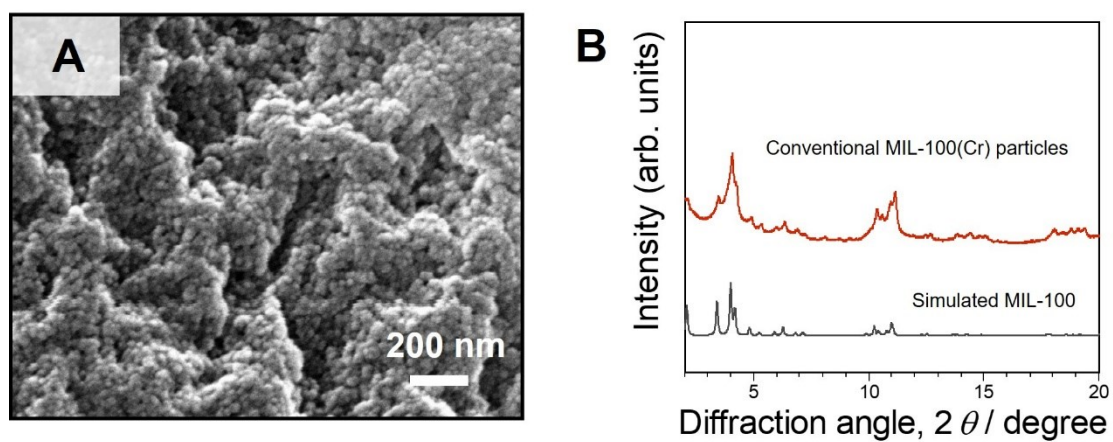


Figure S9. (A) A SEM image and (B) XRD patterns of conventional MIL-100(Cr) particles.

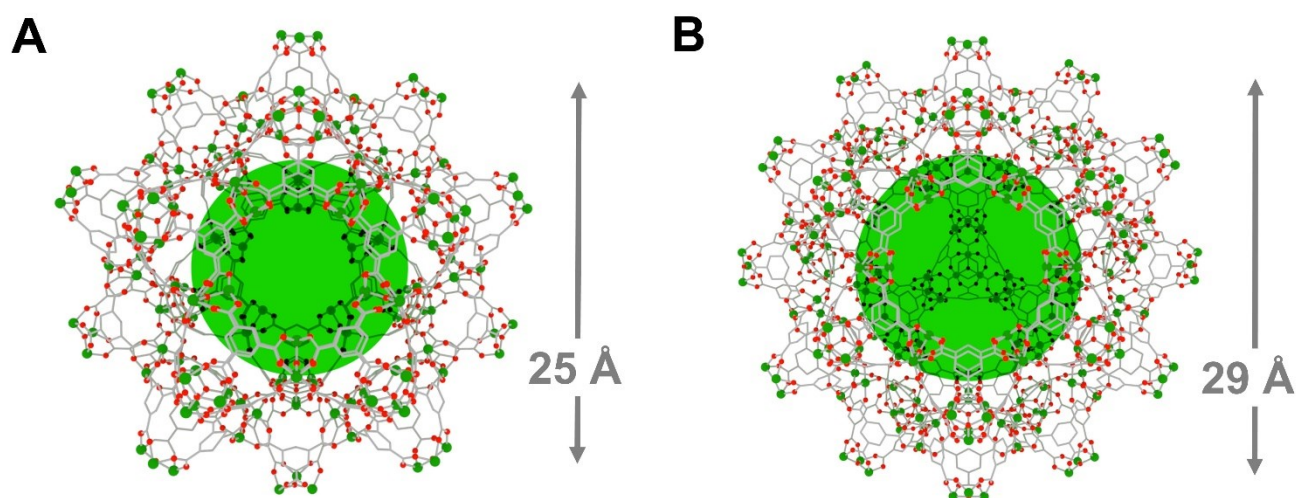


Figure S10. (A,B) Molecular models of MIL-100. MIL-100 has a rigid zeotype structure with two types of cages

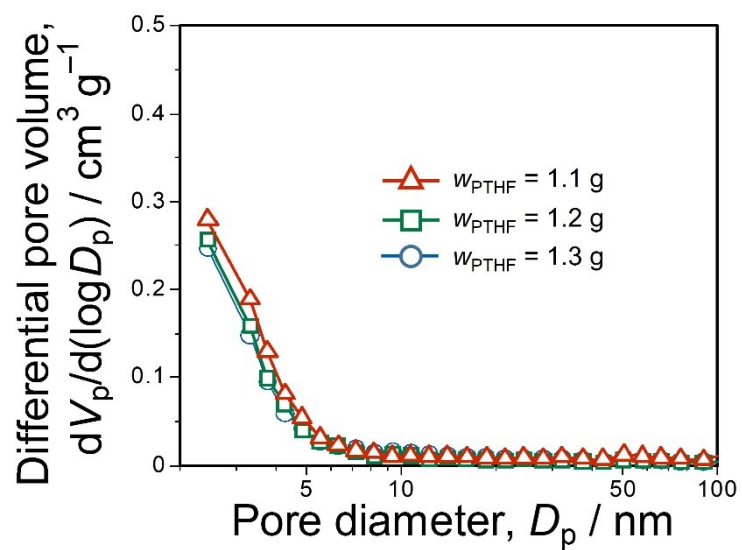


Figure S11. BJH pore size distributions obtained from the adsorption branch of the macroporous Cr-BTC gels with varied amounts of PTHF.

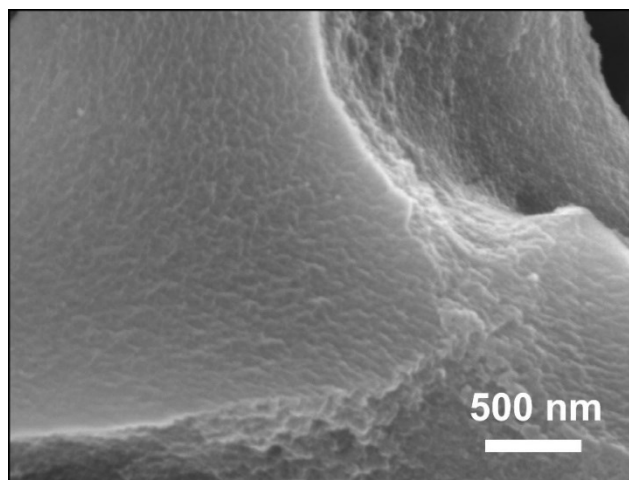


Figure S12. An SEM image of the as-dried macroporous Cr-BTC gel at high magnification: $w_{\text{PTHF}} = 1.2$ g.

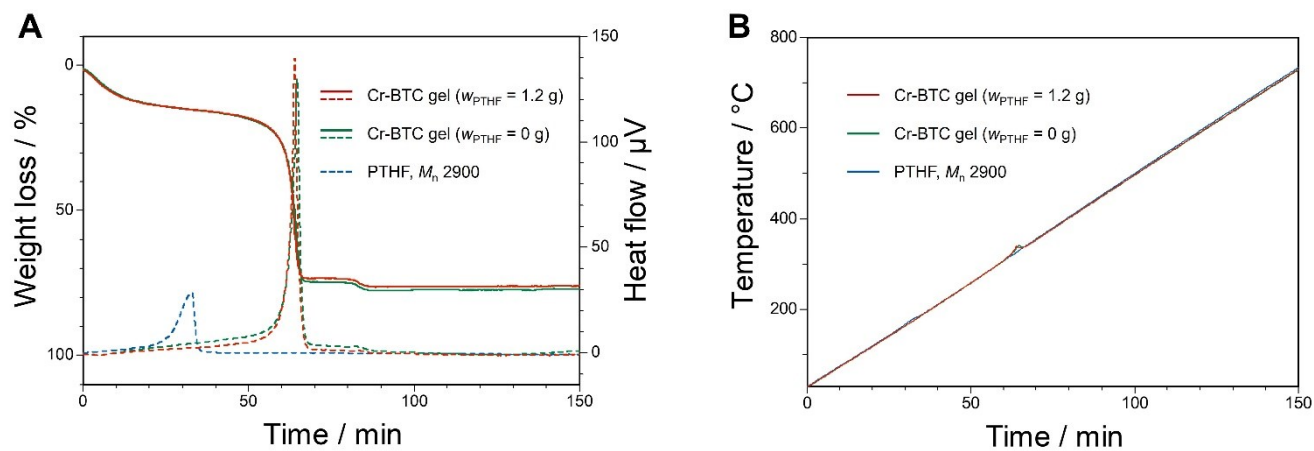


Figure S13. TG and DTA curves of the as-dried macroporous Cr-BTC gel: $w_{\text{PTHF}} = 1.2 \text{ g}$ (red curves) and as-dried non-macroporous Cr-BTC gel: $w_{\text{PTHF}} = 0 \text{ g}$ (green curves), and DTA curve of PTHF $M_n = 2900$ (blue curves).

SUPPLEMENTARY INFORMATION

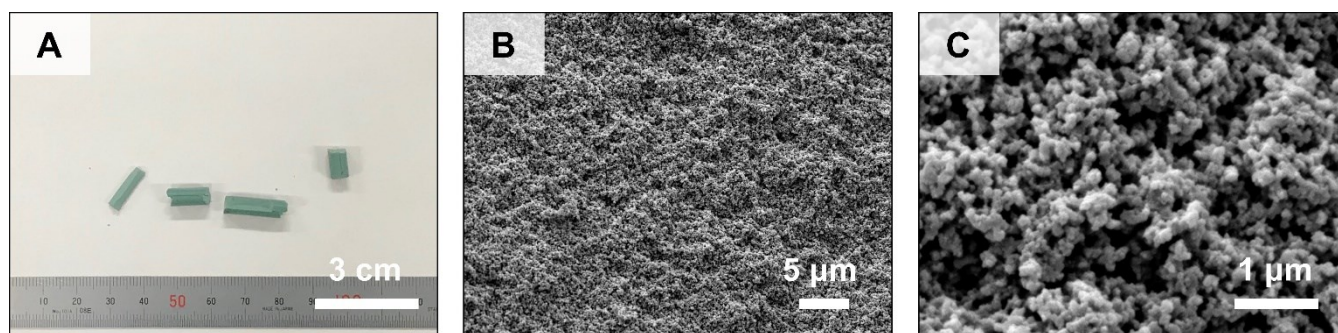


Figure S14. (A) Appearance and (B,C) SEM images of the as-dried macroporous Cr-BTC gels prepared by employing poly(propylene glycol) (PPG, $M_n = 4\,000$) as a phase separation inducer: $w_{\text{PPG}} = 1.3$ g.

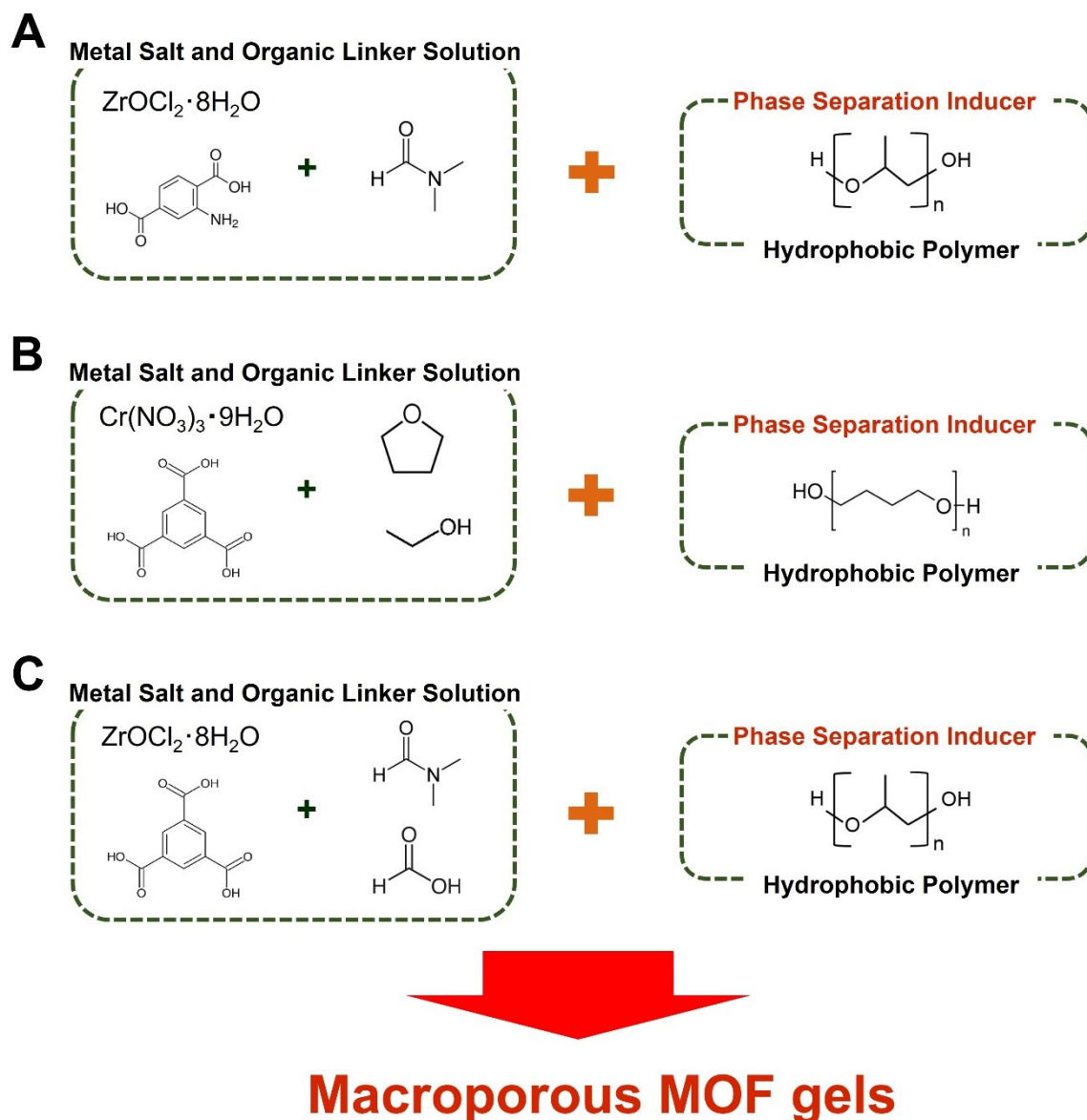


Figure S15. Schematic for the macroporous metal–organic framework gels in different chemical compositions; (A) Zr-BDC-NH₂, (B) Cr-BTC, and (C) Zr-BTC. These three types of macroporous MOF gels have been prepared by employing an appropriate hydrophobic polymer as phase separation inducer.

SUPPLEMENTARY INFORMATION

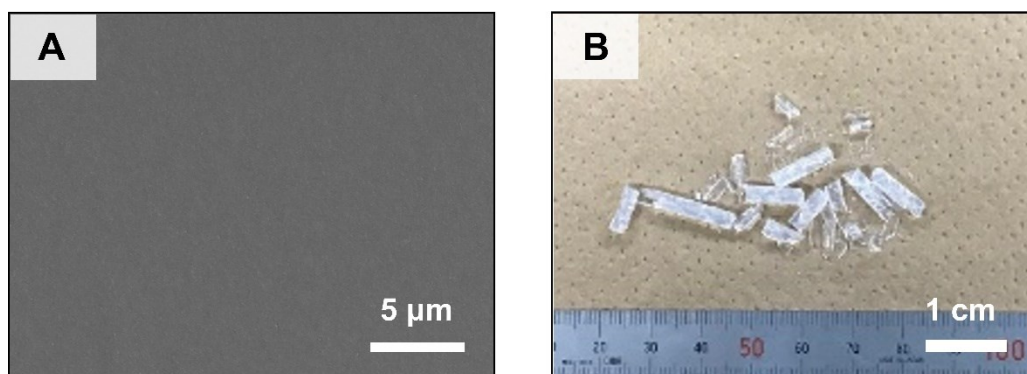


Figure S16. (A) An SEM image and (B) appearance of the as-dried non-macroporous Zr-BTC gels.
 $w_{\text{PPG}} = 0$ mg.

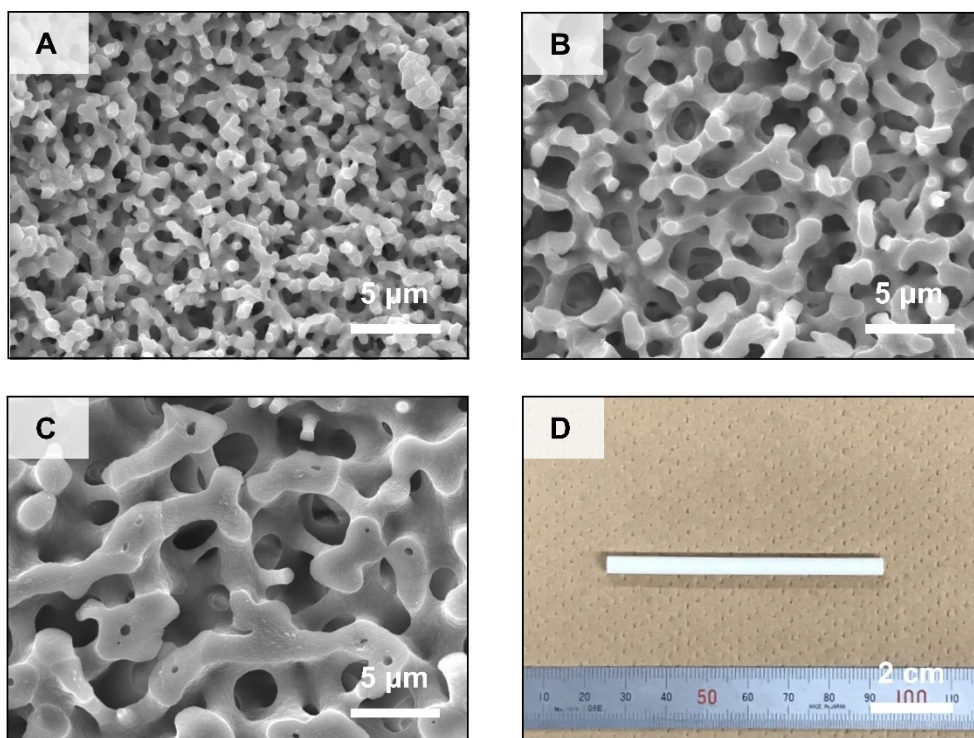


Figure S17. SEM images of the as-dried macroporous Zr-BTC gels prepared with varied amounts of PPG: $w_{\text{PPG}}=A$) 1.16 g, B) 1.18 g, and C) 1.20 g (D) Appearance of the as-dried macroporous Zr-BTC gel. $w_{\text{PPG}} = 1.18$ g.

Figure S17D shows the appearance of the as-dried macroporous Zr-BTC gel. The crack-free monolithic form was preserved during the washing and drying processes.

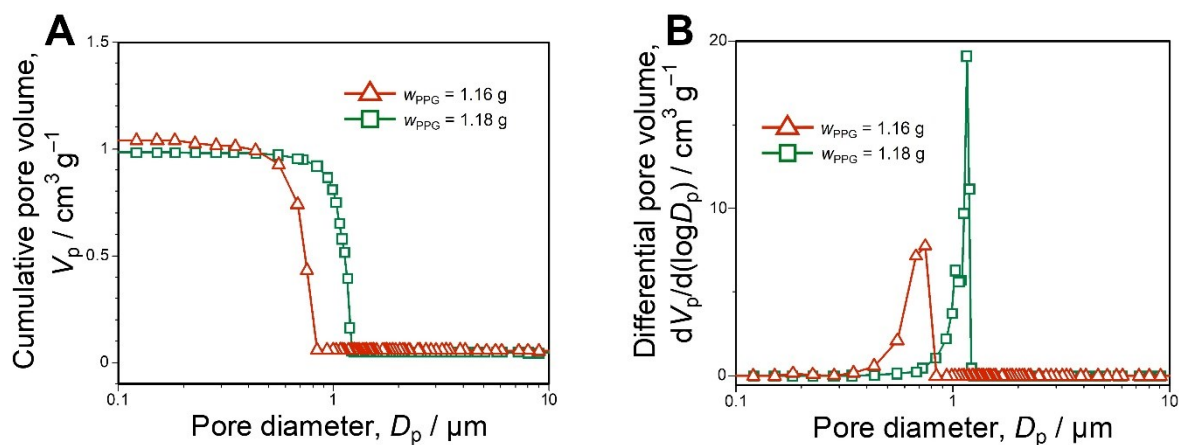


Figure S19. (A) Cumulative and (B) differential pore size distributions of the as-dried macroporous Zr-BTC gels prepared with varied amounts of PPG.

Table S4. Pore properties of the as-dried Zr-BTC gels.

sample	$d_{\text{macro}}^{\text{a}}/\mu\text{m}$	$S_{\text{BET}}^{\text{b}}/\text{m}^2 \text{g}^{-1}$	$V_{(\text{BJH})\text{pore}}^{\text{c}}/\text{cm}^3 \text{g}^{-1}$	$\rho_{\text{b}}^{\text{d}}/\text{g cm}^{-3}$
$w_{\text{PPG}} = 1.16 \text{ g}$	0.75	601	0.20	0.44
$w_{\text{PPG}} = 1.18 \text{ g}$	1.2	586	0.21	0.43
$w_{\text{PPG}} = 1.20 \text{ g}$	-	564	0.20	-

[a] Modal pore size determined by mercury porosimetry. [b] Specific surface area obtained by the BET method. [c] Mesopore volume obtained by BJH method. [d] Bulk density obtained by mercury porosimetry.

Figure S19 shows the mercury intrusion measurements of the macroporous Zr-BTC gels. The macropore diameter was controlled from 0.75 μm to 1.2 μm (**Table S4**). At $w_{\text{PPG}} = 1.20 \text{ g}$, the secondary phase separation ^[1] was observed in the skeletons, and two kinds of macropores were observed (**Figure S18C**).

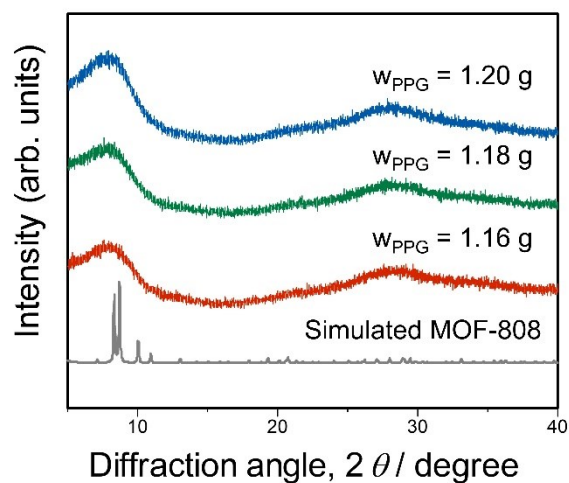


Figure S20. XRD patterns of the as-dried macroporous Zr-BTC gels prepared with varied amounts of PPG.

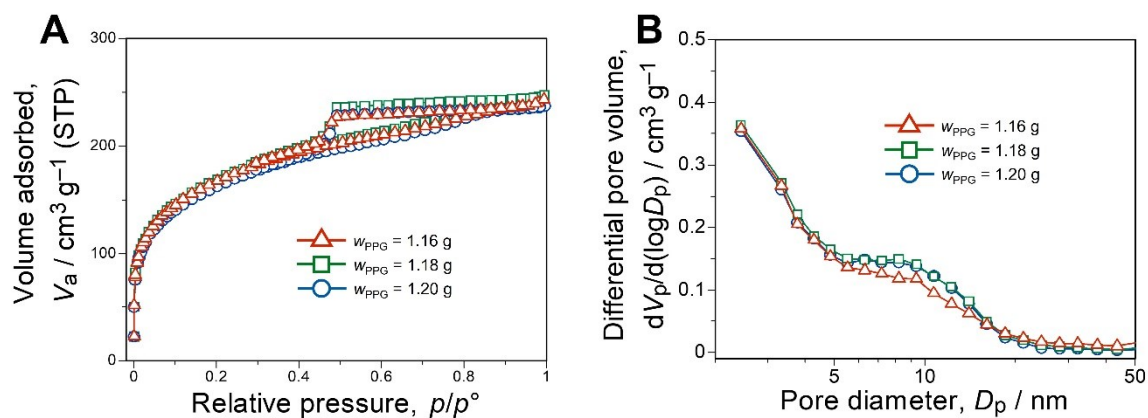


Figure S21. (A) Nitrogen adsorption-desorption isotherms and (B) BJH pore size distributions obtained from the adsorption branch of the macroporous Zr-BTC gels prepared with varied amounts of PPG.

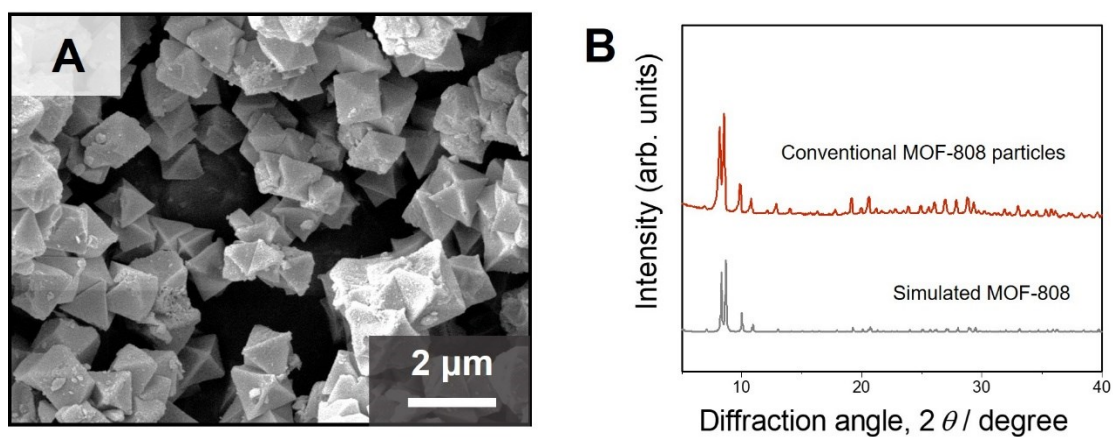


Figure S22. (A) A SEM image and (B) XRD patterns of conventional MOF-808 particles.

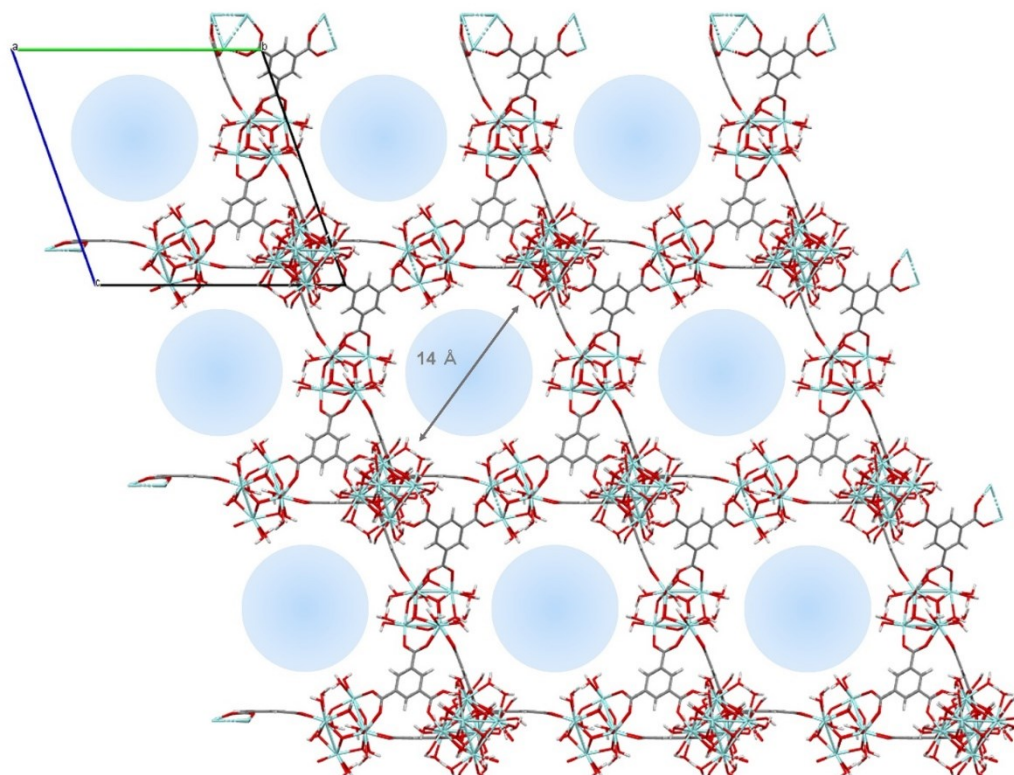


Figure S23. Molecular model of MOF-808.

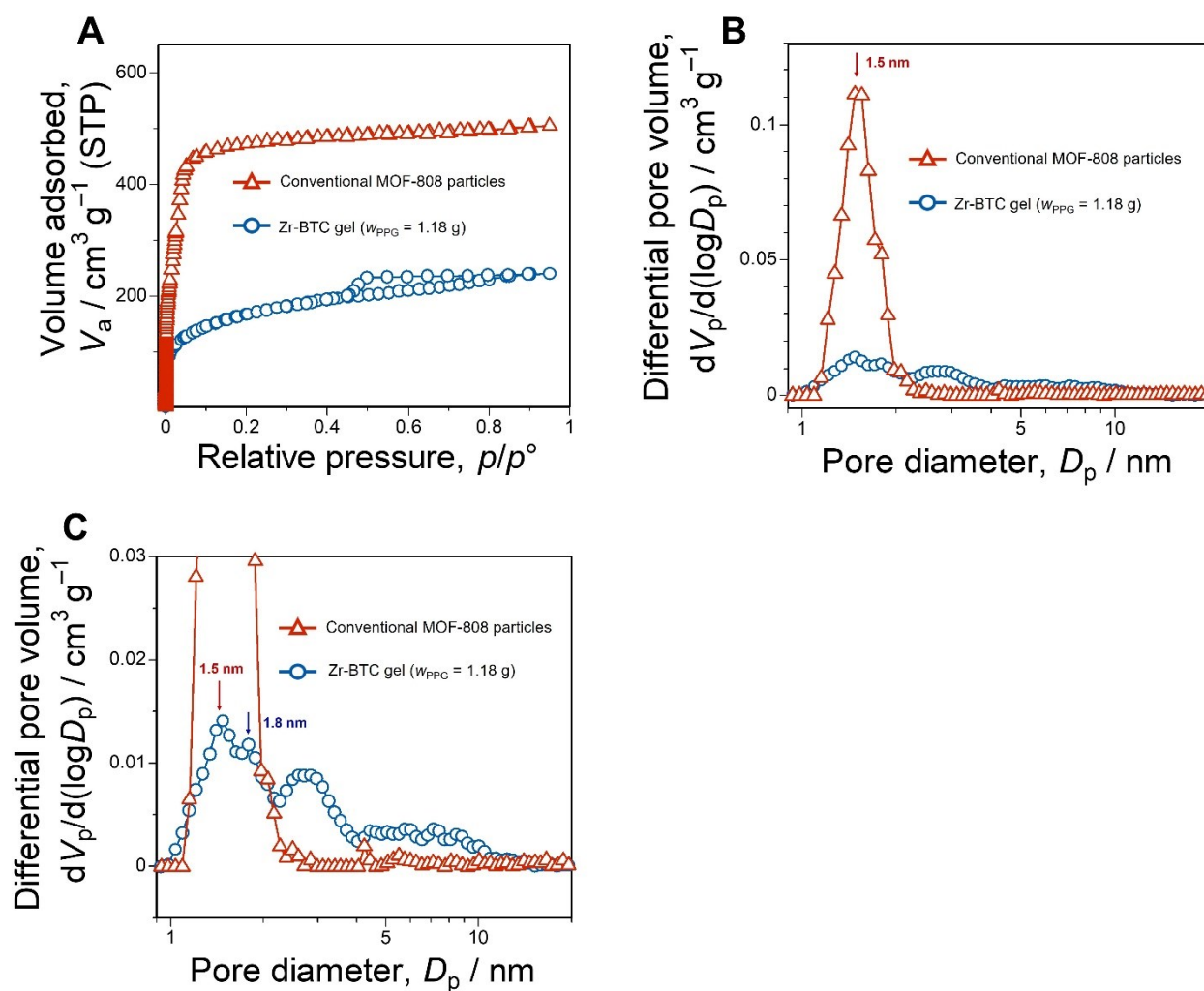


Figure S24. (A) Nitrogen adsorption-desorption isotherms of the samples and (B-C) pore size distributions obtained by the NLDFT analysis. BET surface area of conventional MOF-808 particles are calculated to be $1370 \text{ m}^2 \text{g}^{-1}$.

Figure S20 shows XRD patterns of the as-dried macroporous Zr-BTC gels prepared with varied amounts of PPG. The XRD patterns of the samples show only weak and broad peaks. Although the typical framework structure of Zr-BTC was not detectable, the nitrogen adsorption-desorption results of the Zr-BTC gels show high specific surface area (S_{BET} : 653–661 m² g⁻¹), which suggests the presence of the microporous structures derived from the MOF network (**Figure S21** and **Table S4**). In addition, the micropore size distribution of the samples was estimated by the NLDFT measurements. The pores around 1.4 nm derived from the micropores in the MOF-808 framework (**Figure S23**) can be assigned to be 1.5 nm in the NLDFT pore size distribution of the conventional MOF-808 particles with assumption of N₂-carbon at 77 K on a slit pore model (**Figure S24**). The micropores with a peak at 1.5 nm were also observed in the NLDFT pore size distribution of the Zr-BTC gel (**Figure S24C**). The micropores with a peak at 1.8 nm can be derived from the space between the small crystallite (**Figure S24**). The similar inter-crystallite structure was also observed in the Cr-BTC systems (**Figure 3**). The BJH pore size distributions and isotherms of the Zr-BTC gels indicate the presence of mesopores smaller than 20 nm (**Figure S21B**).

S5. References

- [1] Y. Mao, H. Qi, G. Ye, L. Han, W. Zhou, W. Xu, Y. Sun, *Microporous and Mesoporous Mater.* **2019**, *274*, 70-75.
- [2] H. Furukawa, F. Gándara, Y.-B. Zhang, J. Jiang, W. L. Queen, M. R. Hudson, O. M. Yaghi, *J. Am. Chem. Soc.* **2014**, *136*, 4369-4381.
- [3] K. Nakanishi, *J. Porous Mater.* **1997**, *4*, 67-112.